Influence of Morphological and Electrical Behavior Nano Sized Calcium W-Type Hexaferrites by Chemical Co-Precipitation Technic

Dr. Chandrakant L. Khobaragade
(Department of Physics, Govindrao Wanjari College of Engg & Technology, Nagpur, India)

Abstract: *In the present investigation the samples with chemical composition $CaSr_2(MnZn)_{x/2}Fe_{16-x}O_{27}$, (x = 0, 0.2, 0.4, 0.6, 0.8, 1.0) W-type hexagonal ferrites were synthesized by chemical co-precipitation method. It shows W-type hexagonal crystal structure having unit cell dimensions 'a' varies from 5-6 Å and 'c' varies from 33-34 Å. SEM and TEM study reveals the hexagonal crystal structure of the ferrites. In order to study the electrical behavior of the compound, the room temperature resistivity, activation energy, transition temperature along with Curie temperature (by using Gouy's balance) for all the samples have been carried out.*

Keywords: *XRD, SEM, Electrical conductivity, Activation energy, Curie temperature, Resistivity.*

I. INTRODUCTION

There have been numerous investigations on W-type hexagonal ferrite. These hexagonal ferrites have been a topic of interest due to their high resistivity and low eddy current losses [1-8]. Due to their low eddy current losses, there exist no other materials with such wide ranging values to electronic applications in terms of power generation, conditioning and conversion. A W-type ferrite with chemical composition $AMe_2Fe_{16}O_{27}$, where A represents alkali earth metals, usually Ba, Sr, Ca, Pb etc and Me represents a divalent metal ion, has same crystal structure as that of M-type ferrite except the structural R blocks are separated by two S blocks. The unit cell is composed of sequence R S S R* S* S*, where * represents rotation through 180° [9-13]. W-type hexaferrites are widely used in high density magnetic recording media, overcoat-free, contact or semi-contact recording media and microwave tunable devices working at high frequency, above 70 GHz [14-17]. In CaW-type hexaferrites, the Fe^{3+} ions occupy seven non-equivalent sub-lattices within R-block and S-block, i.e. 12k (R-SS), $4f_2$ (R), 6g (S-S), $4f_2$ (SS) (octahedral coordination), 4e(SS), $4f_1$(SS) (tetrahedral coordination) and 2d(R) (bipyramidal coordination) [18-22]. The magnetic behavior of the compounds has been explained on the basis of interaction amongst the ion occupying these sites. Because of several possible site distributions, various comparative magnetic interactions can arise in the lattice and in turn all these decides magnetic properties of the crystal.

II. EXPERIMENTAL TECHNIC

The calcium W-type hexaferrite were obtained by using chemical co-precipitation method containing AR grade nitrates. Stoichiometric amount of calcium nitrate, zinc nitrate, strontium nitrate, manganese nitrate, ferric nitrate (99.99%) were dissolved one by one in 100 ml of de-ionized water. Ammonia solution (30%) was then added slowly in the mixture to adjust pH of 8. The mixed solution were stirred for two hours and kept at room temperature for 24 hours for aging. The calcium hexaferrite precipitates shall be separated by centrifuged at 2500 rpm for 20 minutes. The prepared precipitate was washed in 1:1 mixture of methanol and acetone followed by 100% de-ionized water to remove impurities. The precipitate was kept for drying at 100℃ for 24 hours. Finally it was calcinated at 1000℃ for 4 hours and grinded in agate pestle-mortar for six hours to obtain CaW-type hexaferrite.

The crystalline structure of the W-type hexaferrites was identified with XPERT-PRO diffractometer at TIFR, Mumbai. The content of the calcium W-type hexaferrite formed at the calcinations stage was estimated from the integral intensity of the diffraction peak. The structural and morphological behavior was studied by Scanning Electron Micrograph (SEM) and Transmission Electron Micrograph (TEM).

The electrical behavior of the compound was studied by graphical representation of logarithmic conductivity with reciprocal of temperature. From this plot the room temperature resistivity, activation energy, transition temperature along with Curie temperature (by using Gouy's balance) for all the samples have been carried out.

III. RESULT AND DISCUSSION

XRD Analysis

The XRD analysis was carried out using XPERT-PRO diffractometer at Tata Institute of Fundamental Research (TIFR), Mumbai. The X-ray powder diffraction pattern of $CaSr_2(MnZn)_{x/2}Fe_{16-x}O_{27}$ for x = 0 is shown in Fig.1. All the reflections can be indexed applying a hexagonal crystal system and space group $P6_3/mmc$, which confirms that the phase belongs to the W-type crystal structure.

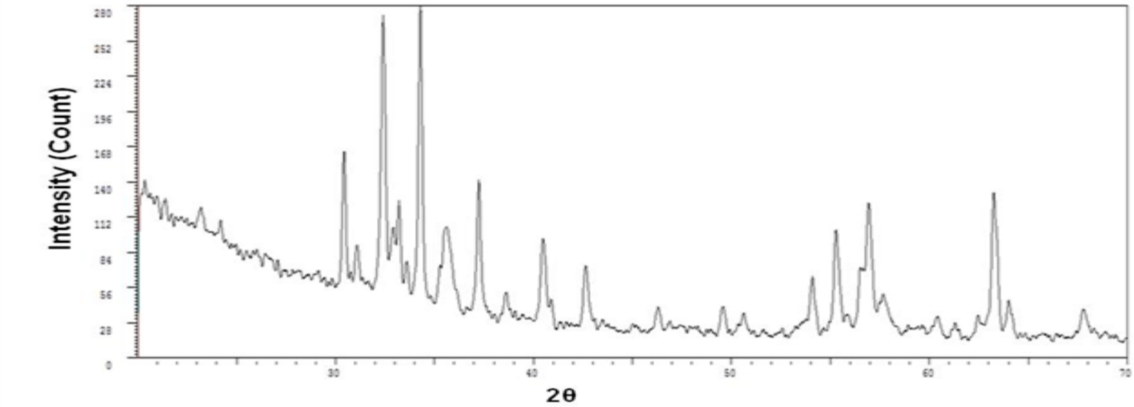

Fig. 1: XRD of compound $CaSr_2(MnZn)_{x/2}Fe_{16-x}O_{27}$ (at x = 0)

The lattice parameter ‘a’ varies from 5.77 Å-5.82 Å and ‘c’ varies from 33.08 Å-33.47 Å shown in Table-1. The structural parameters characterized by lattice constants ‘a’ shows decreasing trend and ‘c’ shows increasing trend with the substitution. This is in agreement with the fact that all hexagonal W-type ferrite exhibit less variation in ‘a’ and ‘c’ [23]. This increase in ‘c’ values may be attributed to the lager ionic radii of Mn (0.67 Å) and Zn (0.74 Å) than iron (0.64 Å).

The crystalline size is obtained from the X-ray diffraction data analysis and it is obtained around 47.67 nm for undoped sample. This crystalline size is found to be decrease with substitution for 0.2 and thereafter increases from 0.4 to 1.0. X-ray density and bulk density shows increasing trend with the substitutions. A very less variation is found in porosity which shows decreasing trend shown in Table-1. The density of Mn and Zn is less than that of Fe. Thus, the addition of Mn-Zn should cause decrease in density of the compound whereas, the increase in density is found with the substitution of dopant. This may be due to the difference in the molecular mass of substituents (Mn = 55, Zn = 65, Fe = 56) [24].

Table-1: Lattice parameters “a” and “c”, volume V, particle size D, X-ray density dx, Bulk density d and Porosity P

Conc x	a (Å)	c (Å)	V (Å^3)	c/a	D (nm)	dx (g/cm^3)	d (g/cm^3)	P
0.0	5.82	33.08	1120.88	5.68	47.67	5.27	2.95	0.44
0.2	5.81	33.10	1117.56	5.70	33.84	5.29	3.06	0.42
0.4	5.79	33.18	1110.91	5.73	36.02	5.32	3.11	0.42
0.6	5.78	33.23	1110.34	5.75	40.18	5.33	3.20	0.40
0.8	5.80	33.23	1116.38	5.73	48.01	5.30	3.30	0.38
1.0	5.77	33.48	1116.18	5.80	41.18	5.31	3.08	0.42

IV. SEM & TEM ANALYSIS

The structure and morphology of the compounds have been studied from the Scanning Electron Micrograph (SEM) and Transmission Electron Micrograph (TEM). The images show clear hexagonal structure of the compound shown in Fig. 2 and Fig. 3. The morphology indicates that the inter grain connectivity gets improved due to substitution. The agglomeration of grains causes increase in size of grain. Also SEM shows the grains of different sizes. This may be due to the different ionic radii of substituent as compared to Fe^{3+} [25].

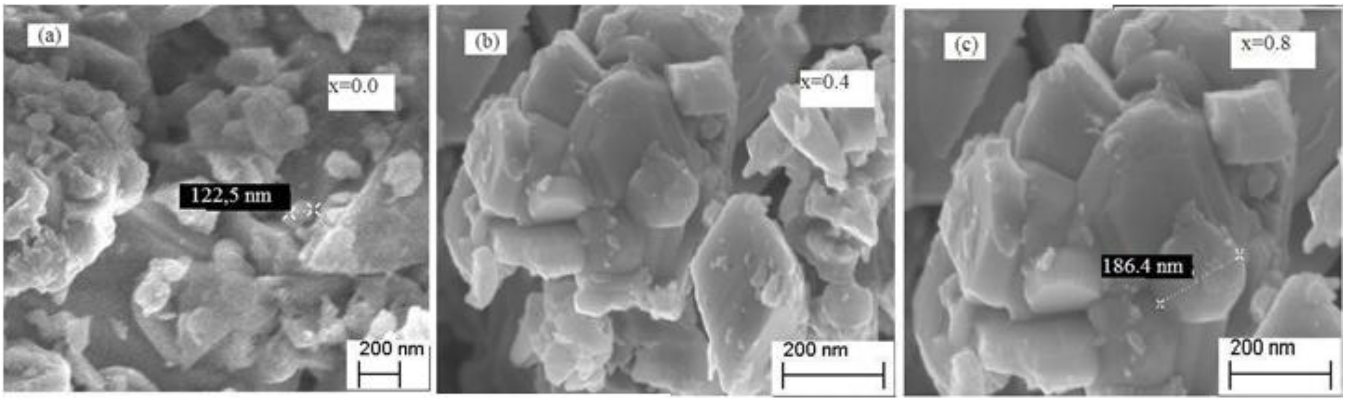

Fig. 2: SEM of $CaSr_2(MnZn)_{x/2}Fe_{16}O_{27}$ compounds at a) x =0.0 b) 0.4 c) 0.8

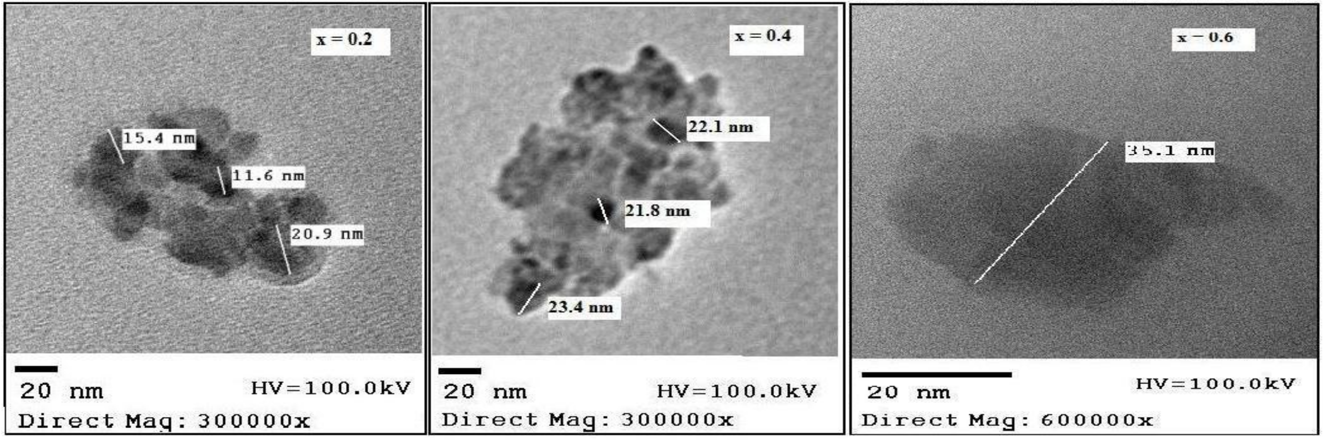

(a) (b) (c)

Fig. 3: TEM Images of $CaSr_2(MnZn)_{x/2}Fe_{16}O_{27}$ compounds at a) x=0.2 b) 0.4 c) 0.6

Electrical Characterization Analysis

In order to study electrical behavior of the compound, the variation of logarithmic conductivity with reciprocal of temperature is studied. The plots showing this behavior are shown in fig.4 (a, b, c, d, e, f). The observed values of room temperature resistivity (RTR), activation energy (E), transition temperature (T_r) along with Curie temperature (T_c) (determined by Gouy's balance) for all the samples are tabulated in Table-2. Increase in value of conductivity with temperature is due to the greater overlap of orbitals owing to increased lattice vibrations. Since the overall distances get reduced during overlap, there will be a greater probability of exchange of charges between the two overlapping ions. Increased exchange due to overlap of orbitals led to increase in the conduction [26]. It is very much clear from the graphs that the conductivity increases with the increase in temperature showing semiconductor behavior of the material. It can be seen that *logσ* increases with that of temperature according to the Arrhenius equation $\sigma = \sigma_0 exp\left(\frac{-E}{kT}\right)$, where E is the activation energy, k is Boltzmann's constant and T is absolute temperature [26-29]. For each sample, there are two regions characterized by transition temperature and having different slopes. This is a magnetic transition from ferrimagnetic to paramagnetic. The transition temperature is found to decrease with the Mn-Zn concentration. The activation energy increases on passing through the transition temperature (Table-2). It may be due to valence exchange mechanism between Fe^{+3} and Fe^{+2} ions [30]. Also increase in activation energy with the Mn-Zn concentration is due to increase in resistivity. The increase in the activation energy after transition temperature may be due to development of oxygen vacancies due to rise in temperature [31]. It may also be due to the change in exchange interaction between A and B sites near Curie point [29]. The transition temperature is found to be nearly equal to Curie temperature.

It is evident from Table-2 that the values of resistivity of the studied compound varies in the range of 5.38×10^5 to 1.43×10^8 Ω-cm. Went *et al* (1952) studied electrical resistivity of polycrystalline and samples of Ba-ferrites [29]. They have reported an approximate value of resistivity of 10^8 Ω-cm at room temperature which corresponds to a value of electrical conductivity of 10^{-8} $\Omega^{-1}cm^{-1}$. Satyanarayana and Murthy (1982) reported Ba/Sr-ferrite with the values from 7.19×10^7 Ω-cm for barium ferrite and 2.26×10^3 Ω-cm for strontium ferrites [32]. Venugopal Reddy and Sheshagiri Rao (1992) reported the electrical resistivity in the range of 10^4 to 10^9 Ω-cm in Li – Ni ferrite system [33].

The increase in room temperature resistivity with Mn-Zn concentration may be due to the high value of resistivity of Mn (144×10^{-8} Ω-m) than Fe (9.61×10^{-8} Ω-m). The cause for increase in resistivity may be the migration of some Fe^{3+} ions from octahedral sites to tetrahedral sites due to substitution. Due to this the concentration of Fe^{3+} ions is lowered in octahedral sites; the site responsible for conduction in ferrites [34]. The increase in resistivity may be due to the fact that Zn^{2+} prefer tetrahedral sites [35-36]. Thus suppress the ferrous formation in the compound.

Table-2: Electrical Parameters $CaSr_2(MnZn)_{x/2}Fe_{16-x}O_{27}$

Conc x	Activation Energy (eV)		R. T. R. (Ω-cm)	T_r (K)	T_c (K)
	Ferri	Para			
0.0	0.382	0.476	5.38×10^5	552.99	561
0.2	0.389	0.467	1.4×10^6	533	529
0.4	0.423	0.557	9.02×10^6	503	500
0.6	0.448	0.628	2.32×10^7	483	478
0.8	0.483	0.662	6.41×10^7	473	470
1.0	0.505	0.705	1.43×10^8	462.99	462

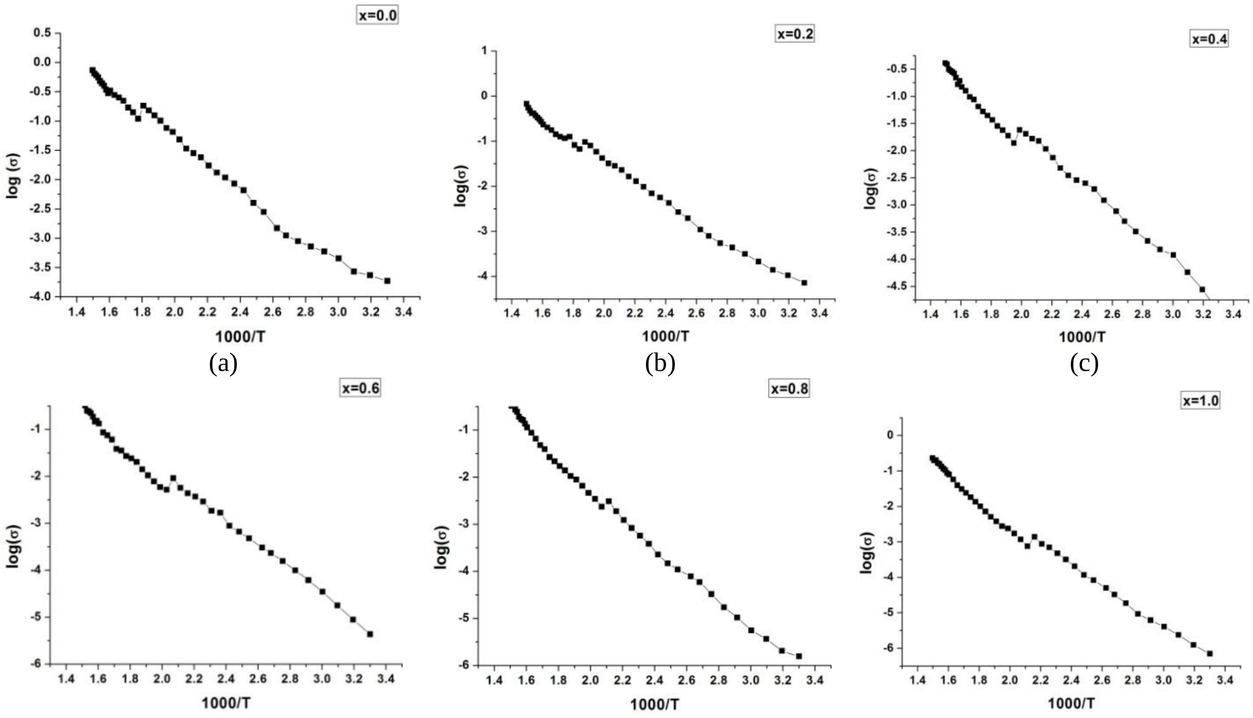

(a) (b) (c)

(d) (e) (f)

Fig 4(a, b, c, d, e, f) : log σ v/s 1000/T for $CaSr_2(MnZn)_{x/2}Fe_{16-x}O_{27}$ (x = 0, 0.2, 0.4, 0.6, 0.8, 1.0

V. CONCLUSION

X-ray density and bulk density of all the compounds increases and porosity shows less variation. SEM and TEM study reveals the hexagonal crystal structure of the ferrites. The derived ferrites have range of particle size distribution with average particle size varies for all compounds from 27.9 nm for $CaSr_2$. The room temperature resistivity showed a gradual increase in the magnitude due to substitution in case of $CaSr_2$ samples. The activation energy for all the samples is found to be different for ferrimagnetic and paramagnetic region. The activation energy in the ferrimagnetic region is observed less than that in paramagnetic region. The transition temperature is found to be nearly equal to Curie temperature which decreases with the increase in impurity conc in the compounds.

VI. REFERENCES

[1] Mukhtar Ahmad, Ihasn Ali, M.U.Islam, Ceramics International, 38(2012) 1267-1273
[2] B. Vishwanatha, V.R.K. Murthy, Ferrite Materials; Science and Technology, Narosa publishing house, New Delhi, U.P. 1990, pp. 429.
[3] E.C. Snelling, Soft Ferrites/Properties and Application; second ed. Butterworths, London, 1988, pp.1.
[4] J. Smith, H.P.J. Wijn, Ferrites, Philips Technical Library, Eindhoven, 1959, pp. 195.
[5] A. Morisako, M. Matsumoto, M. Naoe, IEEE Trans. Magn. M. 3024 (1988)24.
[6] T. L. Hylton, M. A. Parker, M. Ullah, K. R. Coffey, R Umphress, J. K. Haward, J. Appl. Phys.75(1994)5960.
[7] T.P. Niesen, M.R. de Guire, J. Electroceram. M. 169 (2001)6.
[8] M. EL-SAADAWY Journal of Materials Science and Engineering with Advanced Technology Volume 5, Number 2, 2012, Pages 135-151

[9] Mukhtar Ahmad, R. Grossing, Ihsan Ali, Ishtiaq Ahmad, M.U. Rana, Journal of Alloys and Compounds 577 (2013) 382–388
[10] Gagan Kumar, MeenakshiKanthwal, B.S. Chauhan, M Singh, Indian Journal of Pure and Applied Physics, Vol 44, Dec 2006, 930-934
[11] K.J. Standley, Oxide Magnetic Materials (Clarendon Press, Oxford, 1962),p.36.
[12] D.ElKony, S.A. Saafan, A.M. Abo El Ata. Egypt. J. Sol., Vol. (23), No. (1), (2000)13.P.
[13] R. Arjunwadkar, M. Y. Salunkhe, and C. M. DudheHindawi Publishing Corporation Journal of Solid State Physics Volume 2013, Article ID 471472, 6 pages
[14] M.U. Rana, M.U. Islam, UzmaQadri, Journal of Research (Science), BahauddinZakariya University, Multan, Pakistan. Vol.17, No.4, October 2006, pp. 219-224
[15] R. Muller, Journal of Magnetism and Magnetic Materials,101(1991)230-232
[16] C. Surig, K.A. Hempel, R. Muller, P. Gornert, Journal of Magnetism and Magnetic Materials, 150(1995)270-276
[17] M.A. Ahmeda, N. Okasha, R.M. Kershi, Materials Chemistry and Physics 113 (2009) 196–201 [18] M.J. Iqbal, R. A Khan, Shigemi Mizukami, Terunobu Miyzaki, Mat. Research Bull. 46, 1980-1986(2011).
[19] G. Albanese, M. Carbucicchio, G. Asti, Appl. Phys. 11,81088(1976).
[20] A. P. Lilot, A. Gerard, F. Grandjean, IEEE Trans. Magn, 18,1463-1465(1982).
[21] J. Smit, H.P.J. Wijin, Ferrite, Physical Properties of Ferromagnetic Oxides in Relation to their Technical Applications, Wiley, Netherlands, 1959.
[22] F. Leccabue, O. Ares Muzio, M. Safei Eldin Kany, G. Calestani, G. Albanese, J. Mag. Magn. Mat.,68,201-212(1987).
[23] A. K. Akant, C. L. Khobaragade, Research & Reviews: Journal of Physics, Vol.-5, Issue-1, p.g. 1-7 (2016).
[24] Imran Khan, Imran Sadiq, M. N. Ashiq. M. U. Rana, J. Alloys Comp. 509, 8042-8046 (2011).
[25] Charanjeet Singh, S. Bindra Narang, I. S. Hudiara, Yang Bai, Faride Tabatabaci, Mater, Res. Bull., 43, 176-184 (2008).
[26] P.R. Arjunwadkar, M.Y. Salunkhe, C.M. Dudhe, J. Solid State Phys., Hindawi Publishing Corporation(2013).
[27] M.El. Saadawy, JMEAT, 5,135-151(2012).
[28] D.M. Hemeda, O.M. Hemeda, American J. Appl. Sci, 5(4), 289-295(2008).
[29] S.M. Attia, A.M. Abo El Ata, D. El. Kony, J. Mag Magn Mater, 270, 142.151(2004).
[30] Heneda K, Kojima H. Pyhsica Status Solidi (A). ,6: 256p(1971).
[31] Faiza Aen, Shahida B. Niazi, M.U. Islam, Mukhtar Ahmad, M.U. Rana, Ceramic Int., 37,1725-1729(2011).
[32] Satyanarayana R, Murthy S.R. and RaoT.S., J. Less-Common Metals 86 (1982) 115.
[33] Venugopal Reddy and Seshagiri T. Rao, J. of Less Common Metals, 79 (1981) 191-198.
[34] Ali-Sharbati, J.M.V. Khani, G.R. Amiri, R. Mousarezaei, Bill. Mater. Sci, 38, 1-5(2015).
[35] T. Besagni, A. Deriu, F. Licci, S. Rinaldi, J. Mag. Magn. Mater,31, 791-792(1983).
[36] You Lishun, Qiao Liang, ZhengJingwu, Jiang Meiyan, Jiang Liqiang, Sheng Jiawei, J. Rare Earth, 26, 81-84(2008).